Novel diastereoisomers of $C_{21}H_{20}O_3$ obtained from the cathodic reduction of methyl (2E)-3-[2-(2-{2-[(1E)-3-methoxy-3-oxoprop-1-en-1-yl]phenyl}ethyl)phenyl]prop-2-enoate

Ricardo Curilazo,[I] Vera L. Pardini,[I] Hans Viertler,[I] Julio Zukerman-Schpector[*II] and Edward R. T. Tiekink[*III]

[I] Instituto de Química, Universidade de São Paulo, C. P. 26077, 05508-000, São Paulo, SP, Brazil

[II] Departamento de Química, Universidade Federal de São Carlos, Laboratório de Cristalografia, Estereodinâmica e

Modelagem Molecular, C. P. 676, 13565-905, São Carlos, SP, Brazil

[III] Centre for Crystalline Materials, School of Science and Technology, Sunway University, 47500 Bandar Sunway,

Selangor Darul Ehsan, Malaysia

Abstract. The diastereoisomeric title compounds, **5** and **6**, were obtained as a result of intramolecular electrohydrocyclisation of methyl (2E)-3-[2-(2-{2-[(1E)-3-methoxy-3-oxoprop-1-en-1-yl]phenyl}ethyl)phenyl]prop-2-enoate. The common feature of the molecular structures is the presence of a central, eight-membered, –C(H)–C(H)–C⋯C–(CH₂)₂–C⋯C, ring appended to a cyclopentenyl and two phenyl rings. This study represents an unprecedented structural characterisation of such an atomic/bonding arrangement. The distinctive feature of the structures relates to the conformation of the central rings, i.e. approximating a boat in **5** and a chair in **6**. This difference in molecular conformations arises from the different configurations at the methine-C atoms of the cyclopentenyl ring, i.e. *R*- and *S*-(or *S*- and *R*-) in **5** as opposed to *R*- and *R*- (or *S*- and *S*-) in **6**. In each case, the hydroxyl-OH forms an intramolecular hydrogen-bond to the adjacent carbonyl-O atom so the molecular packing in each of **5** and **6** is sustained by non-conventional interactions. A three-dimensional architecture in **5** arises from a combination of phenyl-C–H⋯O(carbonyl) and methyl- and methylene-C–H⋯π contacts. In the crystal of **6**, supramolecular chains with a zig-zag topology along the *c*-axis are formed via methyl-C–H⋯O(hydroxyl); the chains pack with no directional interactions between them.

[*] Correspondence authors: julio@ufscar.br (J.Z.-S.); edwardt@sunway.edu.my (E.R.T.T.)

Introduction

The cathodic reduction of activated alkenes by electron-withdrawing substituents, such as CO_2R, COR, CN, NO_2 and C=NR, is an important carbon-carbon bond formation reaction leading to a reductive coupling product. The kinetic and mechanistic aspects of these coupling reactions are well understood and usually lead to linear, dimeric structures. Under specific experimental conditions, hydrogenation, dimerisation followed by cyclisation or polymerisation may occur leading to different products [1]. Cinnamic acid esters with ring- or double bond-substituents have been studied in this context, and according to the nature of carboxylate group, the formation of a cyclic dimer with a five-membered ring can result by way of a Dieckmann reaction [2-4]. Following this observation, an organic compound that has two 2-alkoxycarbonylvinyl groups in its structure should exhibit similar behaviour to cinnamates. However, when these groups are separated by a bridge that contains double bounds some differences in electrochemical behaviour may be observed. When present, these differences are inherent to the electronic interactions between the two 2-alkoxycarbonylvinyl groups, as apparent for the substrates dialkyl 3,3'-(1,2-, 1,3- and 1,4-phenylene)-bis-(2-propenoates) [5, 6] i.e. **1**, **2** and **3**, respectively, see Fig. 1 for chemical structures. By contrast to **1-3**, the substrate methyl (2E)-3-[2-(2-{2-[(1E)-3-methoxy-3-oxoprop-1-en-1-yl]phenyl}ethyl)-phenyl]-prop-2-enoate (**4**), where no conjugation between the two groups involved in the reductive coupling is possible, the cathodic reduction course must follow a different pathway. Herein, cyclic voltammetry in anhydrous dimethylformaide (DMF) and acetonitrile (MeCN) were performed on substrate **4**. Two of the products, **5** and **6**, were isolated in crystalline form and subjected to X-ray structure determination in order to unambiguously determine the three-dimensional structures as the spectroscopic evidence was inconclusive.
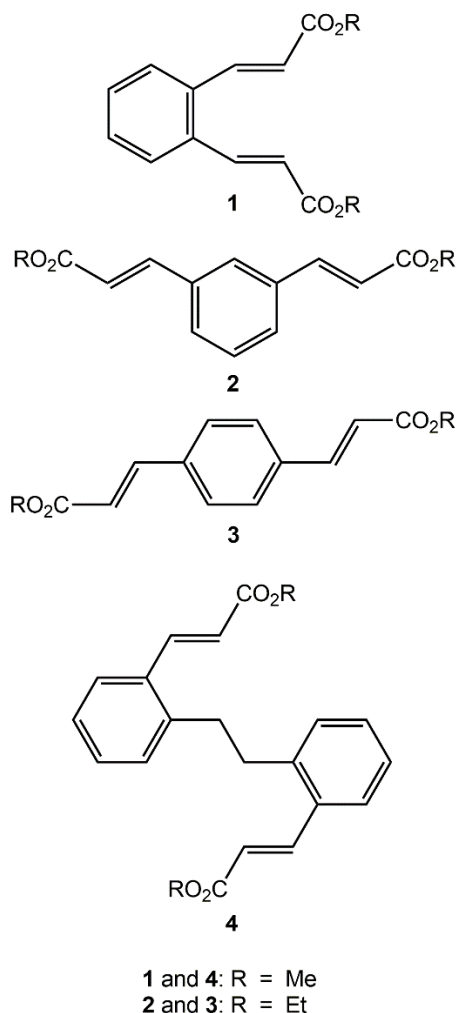
Fig. 1: Chemical diagram for 1-4.

Experimental

Synthesis and characterisation

NMR spectra (^{1}H, ^{13}C, DEPT 135°) were recorded on Bruker AC-200 and DRX-500 spectrometers in CDCl$_3$ solutions with tetramethylsilane (TMS) as the internal standard. When the sample was not soluble in CDCl$_3$, DMSO-d_6 was employed. GC analysis were performed on a HP5890 instrument (fused silica capillary column HP-17, 10m x 0,53mm) and mass spectra (EI) were obtained on a Shimadzu 14B/QP 5050A instrument at 70 eV. Infrared data were obtained on a Perkin-Elmer FT-IR 1750 in CDCl$_3$ solution or as KBr pellets. Elemental analyses were performed on a Perkin-Elmer 2400 instrument. Melting points were performed on a Kofler instrument and are not corrected.

Electrochemical Experiments [2, 3]

Cyclic voltametry experiments were run in a three compartment cell using a Princeton Applied Research 173 potentiostat/galvanostat. The reference electrode was Ag/Ag/I (a silver wire immersed in anhydrous DMF or MeCN/0.1 mol L^{-1} solutions in tetrabutylammonium iodide (TBAI)), freshly electrochemically deposited mercury on a platinum bead as the

working electrode and a platinum foil (4 cm^2) as the counter electrode. Solvents/supporting electrolyte was anhydrous DMF or MeCN/0.1 mol L^{-1} of dry tetraethylammonium perchlorate (TEAP). The substrate concentration was 6.72 mmol of methyl (2E)-3-[2-(2-{2-[(1E)-3-methoxy-3-oxoprop-1-en-1-yl]phenyl}ethyl)phenyl]prop-2-enoate (**4**) and the sweep rate 100 mV s^{-1}. The recorded potential peaks located in the most negative region obtained in DMF (-1.82 V vs Ag/AgI) and MeCN (-1.83 V vs Ag/AgI) were not used because they can involve the reduction of solvent and/or supporting electrolyte molecules. This fact was observed when cyclic voltamograms were run without **4**.

General Procedure for the electrolyses [2, 3]

Methyl (2E)-3-[2-(2-{2-[(1E)-3-methoxy-3-oxoprop-1-en-1-yl]phenyl}ethyl)phenyl]prop-2-enoate (**4**) was electrolysed in a divided cell made of glass equipped with a mercury pool as working electrode, platinum foil as counter electrode and the reference was Ag/AgI as described above In both solvents/supporting electrolytes solutions, the potentials were applied until the current reached 5% of its initial value (20-40 mA). When the solvent employed was anhydrous DMF, the electrolysed solution was diluted with cold, acidified H$_2$O (70 ml; pH 2-3), extracted with ether (3 x 30 ml), washed with saturated NaHCO$_3$ (1 x 30 ml), H$_2$O (3 x 30 ml), saturated NaCl (3 x 30 ml) and dried over MgSO$_4$. In the case of anhydrous MeCN, the excess of MeCN in the electrolysed solution was evaporated under reduced pressure. The residual was dissolved in H$_2$O (100 ml), acidified with dilute HCl (5 % (v/v)) until the pH 2-3. The solution was extracted with ether (3 x 30 ml), washed with saturated solutions of NaHCO$_3$ (1 x 30 ml), H$_2$O (3 x 30 ml) and NaCl (3 x 30 ml), and then dried over MgSO$_4$. The precipitated solids were filtered, dried over P$_2$O$_5$ and submitted to melting point analysis. The solvent was evaporated, the residues stripped off in vacuo and the crude products were submitted to a chromatographic column in silica gel (70-230 mesh) using hexanes (b.pt: 60-68 °C)/ethyl acetate in varying proportions as eluent. The yields of electrolyses products were calculated based on the initial amount of starting material **4**.

Synthesis of starting materials

The starting material methyl (2E)-3-[2-(2-{2-[(1E)-3-methoxy-3-oxoprop-1-en-1-yl]phenyl}ethyl)phenyl]prop-2-enoate (**4**) was synthesised in accord with the procedures detailed below.

Methyl 2-methylbenzoate: 2-Methylbenzoic acid (25.0 g, 184 mmol) and anhydrous methanol (190 ml) were refluxed in the presence of concentrated H$_2$SO$_4$ (10 ml, 5% (v/v)) for 24 h. After cooling, excess methanol was evaporated and the residue diluted in water (120 ml), extracted with ether (3 x 40 ml), washed with aqueous NaHCO$_3$ (1 x 30 ml), H$_2$O (3 x 40 ml), aqueous NaCl (3 x 30 ml) and dried over MgSO$_4$. After the removal of ether, the product was obtained (27.02 g, 98%). ^{1}H NMR (200 MHz, CDCl$_3$, ppm) δ: 2.56 (3H, s); 3.79 (s, 3H); 7.11-7.89 (m, 4H).

Methyl 2-(bromomethyl)-benzoate: A solution of bromine (5.2 ml, 15.98 g, 100 mmol) in CCl$_4$ (100 ml) was slowly added over 5 min to a solution of methyl 2-methylbenzoate (prepared as above) (15.02 g, 100 mmol) in CCl$_4$ (100 ml) with vigorous stirring and then irradiated with a 500 W tungsten lamp. The reaction was considered complete when no more evolution of HBr was observed and the solution became clear. Most of the CCl$_4$ was evaporated and light petroleum (1 ml, b. pt: 30-40 °C) was added to the residue. The solution was cooled in a dry-ice/ethanol bath until complete precipitation of the desired product 19.00 g (83 %). M. pt: 27-29 °C (Lit.

[7]: 28.5-30.0 °C). ^{1}H NMR (200 MHz, CDCl$_3$, ppm) δ: 3.94 (3H, s); 4.96 (2H, s); 7.33-7.99 (4H, m).

Methyl 2-{2-[2-(methoxycarbonyl)phenyl]ethyl}benzoate: Zn[0] activation [8]: 16.40 g (247 mmol) of zinc dust was suspended in H$_2$O (200 ml). To this suspension, a solution of AgNO$_3$ (1.62 g, 9.5 mmol) of in H$_2$O (13 ml) was added. The mixture was heated at 80-90 °C under stirring for 1 h. After cooling, the decanted activated Zn[0] was washed with cold H$_2$O (5 x 50 ml). **Preparation** [9]: To freshly activated Zn[0] was added a portion of H$_2$O (200 ml) and methyl 2-(bromomethyl)-benzoate (see above; 15.0 g, 66 mmol). The mixture was stirred at -90 °C for 4 h after which CH$_2$Cl$_2$ (50 ml) was added with stirring. The mixture was filtered and the residual zinc washed with CH$_2$Cl$_2$ (4 x 50 ml). The organic extracts were combined, washed with NaCl solution (3 x 60 ml) and dried over MgSO$_4$. After CH$_2$Cl$_2$ removal and recrystallisation from methanol, 5.08 g (52 % yield) of the product was obtained as pale-yellow needles. M. pt: 101-102 °C (Lit. [9]: 103 °C). ^{1}H NMR (200 MHz, CDCl$_3$, ppm) δ: 3.26 (4H, s); 3.89 (6H, s); 7.20-7.90 (8H, m).

(2-{2-[2-(Hydroxymethyl)phenyl]ethyl}phenyl)methanol: A solution of methyl 2-{2-[2-(methoxycarbonyl)phenyl]ethyl}benzoate (see above; 5.48 g, 184 mmol) in anhydrous THF (40 ml) was added drop-wise to a stirred suspension of LiAlH$_4$ (3.48 g, 920 mmol) in THF (50 ml). The mixture was refluxed overnight and decomposed with ice and diluted sulfuric acid. The solution was extracted with ether (3 x 70 ml), washed with H$_2$O (3 x 70 ml), NaCl solution (3 x 70 mL) and dried over MgSO$_4$. After solvent removal, 3.88 g of the desired product (87 %) was obtained. M. pt: (EtOH): 147-149 °C, (Lit. [10]: 151 °C). ^{1}H NMR (200 MHz, CDCl$_3$, ppm) δ: 1.97 (1H, s); 3.01 (4H, s); 4.63 (4H, s); 7.25-7,49 (8H, m).

2-[2-(2-Formylphenyl)ethyl]benzaldehyde: (2-{2-[2-(Hydroxymethyl)phenyl]ethyl}phenyl)methanol (see above; 2.18 g, 9.0 mmol) was added in one portion to a vigorously stirred suspension of pyridinium chlorochromate (PCC) [11] (5.83 g, 27 mmol) in anhydrous CH$_2$Cl$_2$ (20 ml). The stirring was continued at room temperature for 90 min. Anhydrous ether (40 ml) was added, decanted and the black residue washed with ether (3 x 30 ml). The combined extracts were filtered through silica gel 70-230 mesh (15.0 g). Solvent evaporation yielded 1.93 g (92%) of the desired product. M.pt (EtOH): 100-102 °C. ^{1}H NMR (200 MHz, CDCl$_3$, ppm) δ: 3.32 (4H, s); 7,27-7,84 (8H, m); 10.20 (2H, s). ^{13}C NMR (50 MHz, CDCl$_3$, ppm) δ: 34.70; 126.79; 131.40; 132.71; 133.76; 143.61; 192.63. GC-MS – EI (m/z) (relative intensity) 238 (0.60); 237 (1.00); 220 (70.00); 209 (1.60); 191 (28.60); 178 (8.70); 165 (10.70); 152 (4.10); 139 (1.30); 132 (8.40); 119 (27.50); 105 (7.20); 91 (100.00); 65 (53.80); 51 (15.40); 39 (21.10). LC-MS – ESI Calc. (M-Na)$^+$: 261.0894; Found (M-Na)$^+$: 261.0886. Elemental analysis: calc. for C$_{16}$H$_{14}$O$_2$.¼H$_2$O: C, 79.44, H, 6.01; O, 14.55. Found C$_{16}$H$_{14}$O$_2$.¼H$_2$O: C, 79.35; H, 6.03; O, 14.62.

(2E)-3-[2-(2-{2-[(1E)-3-Oxoprop-1-en-1-yl]phenyl}ethyl)phenyl]prop-2-enoic acid [12]: In a mixture of absolute pyridine (25.0 ml) and piperidine (1.0 ml) were dissolved the aldehyde (see above; 2.18 g, 9.2 mmol) and dry malonic acid (3.81 g, 36.6 mmol). The mixture was heated at 90-100 °C with stirring for 3 h. After cooling, the solution was acidified with 10% H$_2$SO$_4$ until pH 1-2. After filtration and drying over P$_2$O$_5$, 7.78 g (94 %), the acid was obtained. M. pt: 250-254 °C. ^{1}H NMR (200 MHz, DMSO-d_6, ppm) δ: 2.95 (4H, s); 6.31 (2H, d, J = 15.8 Hz); 7.70 (2H, d, J = 15.8 Hz); 7.07-8.93 (8H, m). Elemental Analysis: calc. for C$_{20}$H$_{18}$O$_4$.5.3H$_2$O: C, 57.52; H, 6.85; O, 35.63; Found C$_{20}$H$_{18}$O$_4$.5.3H$_2$O: C, 57.26; H, 5.17; O, 37.57.

Methyl (2E)-3-[2-(2-{2-[(1E)-3-methoxy-3-oxoprop-1-en-1-yl]phenyl}ethyl)phenyl]prop-2-enoate (4): To dry benzene (100 ml) were added the acid (see above; 5.0 g, 15.5 mmol) and of thionyl chloride (6.7 ml, 93 mmol). The mixture was refluxed under stirring for 4 h. The benzene was removed by evaporation under reduced pressure and anhydrous methanol (15 ml) added. Refluxing was continued for 2 h. Excess of methanol was evaporated, the residue diluted in H_2O (120 ml, extracted in CH_2Cl_2 (3 x 40 ml), washed with aqueous $NaHCO_3$ solution (1 x 30 ml), H_2O, (3 x 40 ml), aqueous NaCl (3 x 40 ml) and dried over $MgSO_4$. The crude ester **4** was purified by recrystallisation from hot ethanol. After drying over P_2O_5 4.07 g (75%) of **4** was obtained. M. pt (EtOH): 100-102 °C. ^1H NMR (200 MHz, $CDCl_3$, ppm) δ: 3.01 (4H, s); 3.79 (6H, s); 6.35 (2H, d, J = 16.0 Hz); 7.07-7.50 (8H, m); 7.81 (2H, d, J = 16.0 Hz). ^{13}C NMR (50 MHz, $CDCl_3$, ppm) δ: 34.79; 51.51; 118.98; 126.42; 126.72; 130.01; 130.22; 133.18; 140.24; 141.64; 167.16. NMR DEPT 135° (50 MHz, $CDCl_3$, ppm) δ: 25.68; 42.39; 109.85; 117.31; 117.59; 120.90; 121.11; 132.50. FTIR (KBr): 3067; 1709; 1636; 1177; 1020; 977; 863; 764 cm^{-1}. GC-MS – EI (m/z) (relative intensity): 350 (0.90); 318 (2.20); 290 (7.50); 276 (5.00); 258 (2.60); 245 (2.70); 231 (9.50); 216 (20.40); 202 (4.20); 189 (1.00); 175 (1.80); 161 (2.20); 143 (4.60); 129 (9.30); 115 (100.00); 91 (18.10); 77 (4.10); 59 (27.70); 45 (3.30). Elemental Analysis: calc for $C_{22}H_{22}O_4$: C, 75.41; H, 6.33; O, 18.26; Found $C_{22}H_{22}O_4$: C, 75.41; H, 6.10; O, 18.49.

Crystal structure determination

Intensity data for **5** (methyl (2R,6S)-4- hydroxytetracyclo[13.4.0.0^{2,6}.0^{7,12}]nonadeca- 1(15),3,7(12),8,10,16,18- heptaene-3-carboxylate) and **6** (methyl (2S,6S)-4- hydroxytetracyclo[13.4.0.0^{2,6}.0^{7,12}]nonadeca- 1(15),3,7(12),8,10,16,18-heptaene-3-carboxylate) were measured at 98 K on a Rigaku AFC12κ/SATURN724 diffractometer using with MoKα radiation. Data processing and absorption corrections were accomplished with CrystalClear [13] and ABSCOR [14], respectively. Details of cell data, X-ray data collection, and structure refinement are given in Table 1. The structures were solved by direct-methods [15]. Full-matrix least squares refinement on F^2 with anisotropic displacement parameters for all non-hydrogen atoms was performed [16]. The C-bound H atoms were placed on stereochemical grounds and refined with fixed geometries, $U_{iso}(H) = 1.2-1.5 U_{iso}$(carrier atom). The O-bound H atoms were found in difference map and refined with O–H = 0.84±0.01 Å with $U_{iso} = 1.5 U_{eq}(O)$. A weighting scheme of the form $w = 1/[\sigma^2(F_o^2) + (aP)^2 + bP]$ where $P = (F_o^2 + 2F_c^2)/3$ was introduced in each case. The programs WinGX [17], ORTEP-3 for Windows [17], PLATON [18], DIAMOND [19] and QMol [20] were also used in the study.

Tab. 1: Crystallographic data and refinement details for **5** and **6**.[1]

	5	**6**
Formula	$C_{21}H_{20}O_3$	$C_{21}H_{20}O_3$
Formula weight	320.37	320.37
Crystal colour, habit	pale-rose, prism	colourless, plate
Crystal size/mm	0.19 x 0.30 x 0.32	0.02 x 0.20 x 0.25
Crystal system	triclinic	monoclinic
Space group	$P\bar{1}$	$P2_1/c$
a/Å	7.942(2)	10.238(7)
b/Å	8.6535(18)	15.269(9)
c/Å	12.453(3)	10.593(7)
α/°	69.969(7)	90

$\beta/°$	87.862(12)	102.357(10)
$\gamma/°$	85.333(12)	90
$V/\text{Å}^3$	801.3(3)	1617.7(18)
Z/Z'	2/1	4/1
$D_c/\text{g cm}^{-3}$	1.328	1.315
$F(000)$	340	680
$\mu(\text{Mo}K\alpha)/\text{mm}^{-1}$	0.088	0.087
Measured data	6071	9984
θ range/°	2.5-27.5	2.4-25.0
Unique data	3655	2814
R_{int}	0.040	0.039
Observed data ($I \geq 2.0\sigma(I)$)	3345	2248
R, obs. data; all data	0.051; 0.055	0.086; 0.102
a; b in wghting scheme	0.056; 0.415	0.138; 1.639
R_w, obs. data; all data	0.124; 0.128	0.224; 0.243
Largest difference peak and hole (Å^{-3})	0.30, -0.19	0.43, -0.34

[1] Supplementary Material: Crystallographic data (including structure factors) for the structures reported in this paper have been deposited with the Cambridge Crystallographic Data Centre as supplementary publication numbers CCDC-1533636 and 1533637. Copies of available material can be obtained free of charge, on application to CCDC, 12 Union Road, Cambridge CB2 1EZ, UK, (fax: +44-(0)1223-336033 or e-mail: deposit@ccdc.cam.ac.uk).

Results and discussion

Chemistry

Cyclic voltammetry experiments in anhydrous DMF and MeCN were performed on the substrate methyl (2E)-3-[2-(2-{2-[(1E)-3-methoxy-3-oxoprop-1-en-1-yl]phenyl}ethyl)phenyl]prop-2-enoate (**4**). These experiments showed the presence of an irreversible reduction peak located at -1.42 V (vs Ag/AgI) in each solvent. The potential of the current peaks were consistent [21] with the absence of electronic interactions between the 2-methoxycarbonylvinyl groups indicating that these are not conjugated, as indicated in the chemical diagram of **4**, Fig. 1. In previous studies with **1-3**, where electronic communications are observed between the substituents, the corresponding cyclic voltamograms showed the presence of two reversible reduction waves separated by a difference of approximately 300 mV. For these compounds, the reduction occurs at only at one of the two 2-alkoxycarbonylvinyl groups [2, 22]. As expected for the substrate **4**, where there is no communication between the substituents, during the preparative electrolysis at the controlled potential (-1.42 V vs Ag/AgI) in DMF and MeCN, both groups were concomitantly reduced, an observation confirmed by the consumed charges at the end of experiments, i.e. from 1.75 to 1.86 F, with the values close to 2.0 F corresponding to a two-electron transfer process at the electrode surface. The initial analysis of the compounds separated from the crude mixture after electrolyses in each solvent led only to a partial structural elucidation, Fig. 2. For example, the ^{1}H NMR data indicated the presence of a signal at 11.00 ppm (from CDCl$_3$/TMS) which disappeared in the presence of D$_2$O, being characteristic behaviour of a hydroxyl group. In addition, the ^{13}C NMR experiments showed the presence of two signals corresponding to carbons involved in a double bond, i.e. located at 102.20 ppm (HO-$\underline{C}$=) and 169.70 ppm (=$\underline{C}$-CO$_2$Me). Both facts suggested the presence of a five-membered enolic ring. However, the complexity of signals in the ^{1}H NMR spectra corresponding to the methyl- and methylene-protons in the region 2.68 to 4.13 ppm precluded unambiguous structure assignment. Thus, each isolated sample was dis-

solved in a mixture of methanol/CHCl₃ ((9:1) (v/v)) and after slow evaporation were obtained in crystalline form, then subjected to X-ray structural analysis. In addition to **5** and **6**, the acid (2E)-3-[2-(2-{2-[(1E)-2-carboxy-eth-1-en-1-yl]phenyl}ethyl)phenyl]prop-2-enoic acid) (16-25%) was found (the structure was confirmed by the values of the coupling constants in the ^{1}H NMR) as well as oligomeric products (21-31%) which were not characterised, Fig. 2.
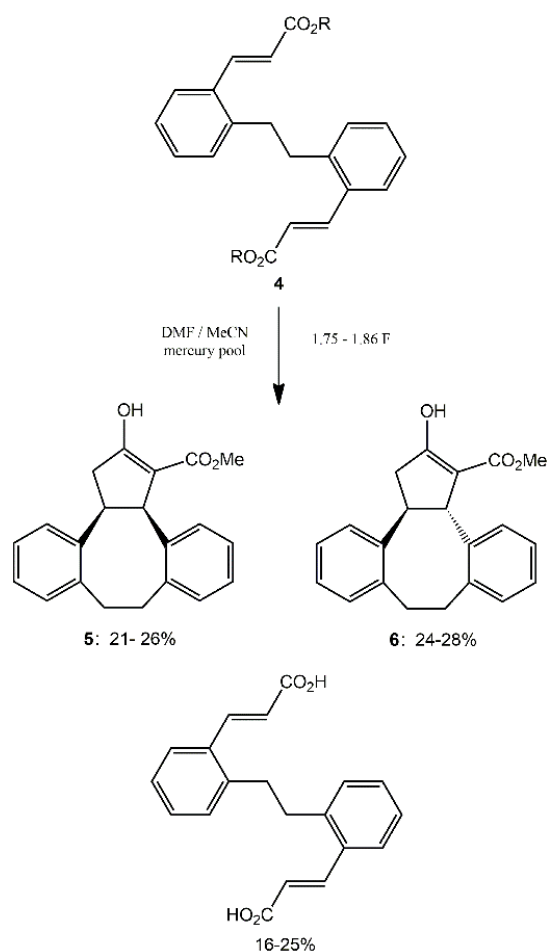

Fig. 2: Outline of the electrochemical synthesis of **5** and **6**, and the known side-product, (2E)-3-[2-(2-{2-[(1E)-2-carboxyeth-1-en-1-yl]phenyl}ethyl)phenyl]prop-2-enoic acid.

Molecular structures

The structure determinations of the products isolated from the intramolecular electrohydrocyclisation mediated by the electrochemical reduction of methyl (2E)-3-[2-(2-{2-[(1E)-3-methoxy-3-oxoprop-1-en-1-yl]phenyl}ethyl)phenyl]prop-2-enoate (**4**), i.e. diastereoisomeric **5** and **6**, were performed in order to assign the molecular structures.

The molecular structure of **5** is illustrated in Fig. 3a. The molecule comprises four fused rings and is constructed about a central, eight-membered ring, C6, C7, C8, C13, C14, C15, C16 and C21, which has a twisted-boat conformation. In this description, the pairs of atoms derived from the phenyl rings, i.e. C8 and C13, and C16 and C21, lie above the approximate plane defined by the sp³-carbon atoms, i.e. C6, C7 C14 and C15. The dihedral angles between the four atoms comprising the base of the boat [r.m.s. deviation = 0.181 Å] and the (C8-C13) and (C16-C21) phenyl rings are 55.17(6) and 52.59(8)°, respectively, and the angle between the two phenyl

rings is 72.25(4)°, Table 2. The five-membered ring, cyclopentene ring adopts an envelope conformation with the flap atom, C6, lying 0.459(2) Å out of the plane defined by the remaining atoms [r.m.s. deviation = 0.000 Å]. The skewed nature of the conformation is reflected in the disparate dihedral angles formed between the cyclopentenyl and C8- and C16-pehnyl rings of 80.25(5) and 27.52 (8)°, respectively. To a rough approximation, the five-membered ring lies above the plane of the base of the central boat, forming a dihedral angle of 31.46(11)°, however, there are significant twists in each plane. The ester residue is essentially co-planar with the five-membered ring as seen in the values of the O1–C2—C3–C4 and O2–C2–C3–C7 torsion angles of 1.0(2) and -0.7(2)°, respectively. The conformation of the carbonyl- and hydroxyl-oxygen atoms is syn, an arrangement that allows an intramolecular hydroxyl-O3–H···O1(carbonyl) hydrogen-bond to form, Table 3.
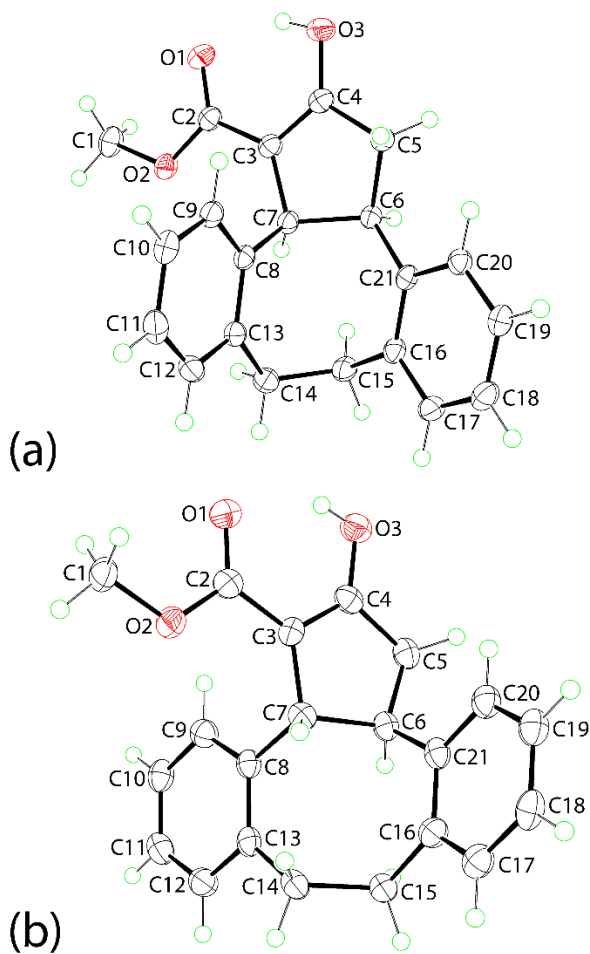

Fig. 3: Molecular structures of (a) **5** and (b) **6**. The dashed lines indicate intramolecular O–H···O hydrogen bonds. Displacement ellipsoids are drawn at the 50% probability level.

Tab. 2: Selected geometric parameters (Å, °) for **5** and **6**.

	5	**6**
Deviations from the least-squares plane through atoms C6, C7, C14 and C15		
C6:	0.1791(8)	-0.081(16)
C7:	-0.1780(8)	0.081(16)
C14:	0.1826(8)	-0.082(17)
C15	-0.1838(8)	0.083(17)
Dihedral angles		

(C6, C7, C14, C15) / (C8-C13)	55.17(6)	58.83(110)
(C6, C7, C14, C15) / (C16-C21)	52.59(8)	68.04(11)
(C3-C7) / (C8-C13)	80.25(5)	70.70(11)
(C3-C7) / (C16-C21)	27.52 (8)	79.99(11)
O1–C2–C3–C4	1.0(2)	1.4(5)
O2–C2–C3–C7	-0.7(2)	-1.0(5)

The molecular structure of **6** is shown in Fig. 3b from which it can be seen that i) the molecular connectivity is as for **5** and ii) a major conformational change in the central eight-membered ring has occurred. The central ring now has the shape of a chair. While the dihedral angles between the central C6, C7, C14 and C15 atoms [r.m.s. deviation = 0.082 Å] and the pendent phenyl rings are, to a first approximation, the same as for **5**, Table 2, the different conformation is best reflected in the dihedral angle between the phenyl rings, i.e. 12.89(18)°, indicating an almost parallel disposition cf. the near orthogonal relationship in **5**, Table 2.

The cyclopentenyl ring in **6** again adopts an envelope conformation with the C6 atom, the flap atom, lying 0.248(3) Å out of the plane defined by the remaining atoms [r.m.s. deviation = 0.005 Å]. Reflecting the different conformation of the central ring in **6**, the both dihedral angles formed between the cyclopentenyl ring and phenyl rings approach orthogonality as opposed to the situation in **5**, Table 2. The relative dispositions of the ester and hydroxyl groups in **6** are as for **5**, Table 2, and the intramolecular hydroxyl-O3–H⋯O1(carbonyl) hydrogen-bond persists, Table 4.

The differences between the molecular structures for **5** and **6** are highlighted in the overlay diagram shown in Fig. 4. From this it is evident that the there is a high degree of coincidence in the substituted cyclopentenyl residues and the significant difference in the conformation of the eight-membered ring. Also evident is the different configurations of the two chiral centres of the cyclopentenyl ring. Referring to Fig. 4, in **5**, the C6 atom has an *R*-configuration and that of the adjacent C7 atom, an *S*-configuration. This has the consequence that the hydrogen atoms of these centres are syn. In the inverted form of **6** shown in Fig. 5, both C6 and C7 have *S*-configurations.
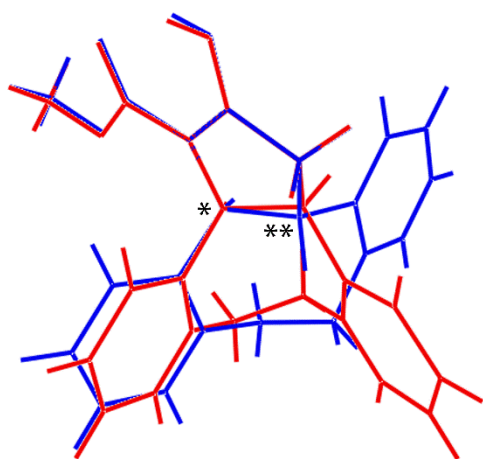

Fig. 4: Overlay diagrams of **5** (red image) and inverted form of **6** (blue). The molecules have been superimposed so that the planar regions of the cyclopentenyl rings are coincident. The centre indicated with an asterisk corresponds to the C6 atom and that with two asterisks, to C7.

Given the different conformations about the central rings in **5** and **6**, i.e. boat and chair, respectively, it was thought of interest to ascertain information concerning the physiochemical properties of the molecules. Thus,

referring to Table 3, the volume, surface area, globularity and asphericity of the molecules were calculated using Crystal Explorer [23], and the density and packing index were calculated using PLATON [18]. The crystal density and packing efficiency for **5** are marginally greater than for **6**. This is consistent with the volume and surface area being smaller, and the slightly greater inclination towards a globular molecule in **5**.

Tab. 3: Physiochemical properties for **5** and **6**.

Property	5	6
Volume, V (A^3)	393.95	397.74
Surface area, A (A^2)	341.25	345.33
$A{:}V$ (A^{-1})	0.87	0.87
Globularity, G	0.762	0.757
Asphericity, Ω	0.086	0.059
Density (g cm^{-1})	1.328	1.316
Packing index (%)	70.9	70.7

A search of the Cambridge Structural Database [24] reveals only two examples of an eight-membered ring appended to a saturated five-membered ring, i.e. with the sequence of bonds within the ring –C(H)–C(H)–C$\cdots$C–(CH$_2$)$_2$–C$\cdots$C. In each of these closely related compounds, the eight-membered ring has a boat conformation, as in **5** [25]. There are no examples included in the CSD of the five-membered ring having a double bond as in **5** and **6** pointing to the novelty of the molecular frameworks reported herein.

Molecular packing

The molecular packing of **5** is dominated by weak interactions. As well as participating in an intramolecular hydroxyl-O3–H$\cdots$O1(carbonyl) hydrogen-bond, the carbonyl-O1 atom also accepts an interaction from phenyl-C17–H; geometric details describing the intermolecular interactions in **5** and **6** are given in Table 4. There is also a relatively close methylene-C6–H$\cdots$π(C16-C21) contact [26] which, when combined with the C–H$\cdots$O contacts, leads to supramolecular layers in the *ab*-plane. Further stabilisation to the layer is afforded by methyl-C–H$\cdots$π(C16-C21) interactions indicating the (C16-C21) ring accepts two such contacts. The layers inter-digitate along the *c*-axis and the connections between them are of the type methylene-C14–H$\cdots$π(C8-C13) so that a three-dimensional architecture ensues, Fig. 5.
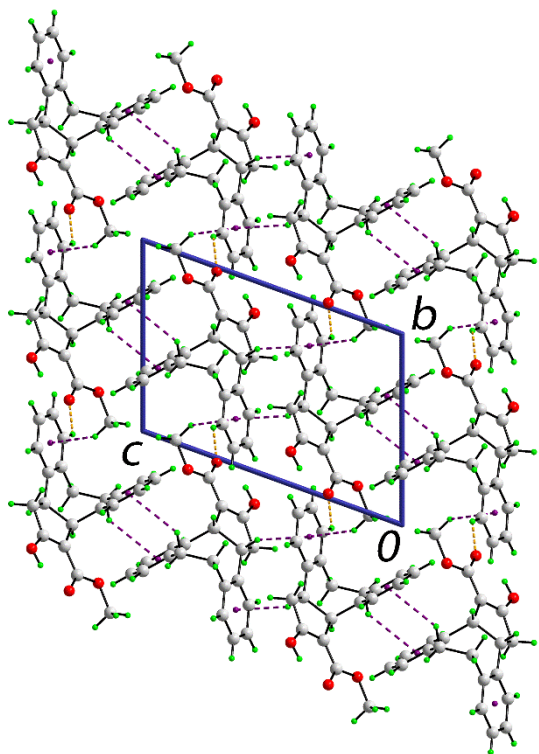
Fig. 5: Molecular packing in **5**: view of the unit cell contents shown in projection down the *a*-axis. The C–H⋯O and C–H⋯π interactions are shown as orange and purple dashed lines, respectively.

In keeping with the distance criteria in PLATON [18], the molecular packing of **6** features less specific interactions than observed in **5**. In addition to the hydroxyl-O3–H⋯O1(carbonyl) hydrogen-bond, the only other directional interaction is a weak methyl-C1-H⋯O(hydroxyl) contact, Table 4. These lead to supramolecular zig-zag chains along the *c*-axis, i.e. propagated by glide symmetry, Fig. 6a. The chains pack with no directional interactions between them, Fig. 6b.
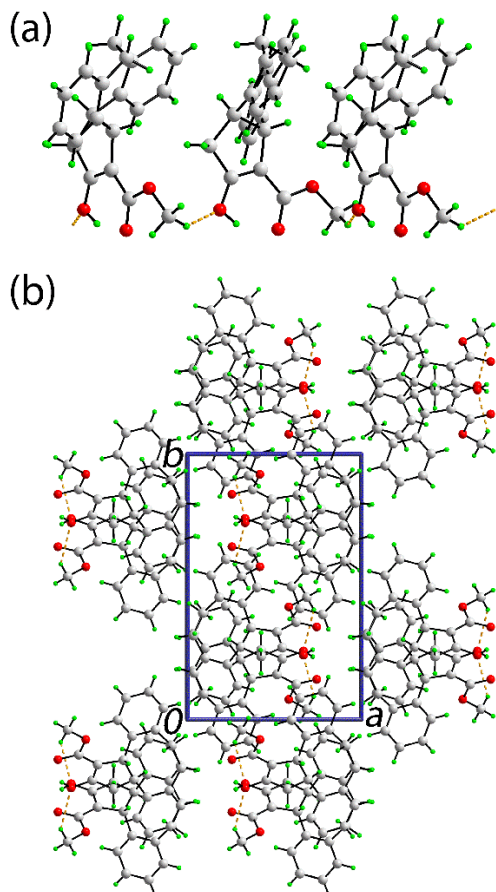
Fig. 6: Molecular packing in **6**: (**a**) detail of the methyl-C–H···O(hydroxyl) interactions, shown as orange dashed lines, leading to a supramolecular zig-zag chain and (**b**) view of the unit cell contents shown in projection down the *c*-axis.

Tab. 4: Summary of intermolecular interactions (A–H⋯B; Å, °) operating in the crystal structures of **5** and **6**.

A	H	B	A–H	H⋯B	A⋯B	A–H⋯B	Symmetry operation
5							
O3	H3o	O1	0.846(19)	1.89(2)	2.6434(19)	148(2)	*x, y, z*
C17	H17	O1	0.95	2.44	3.224(2)	139	*-1+x, 1+y, z*
C6	H6	Cg(C16-C21)	1.00	2.56	3.4802(18)	153	*1-x, 1-y, 1-z*
C1	H1c	Cg(C16-C21)	0.98	2.96	3.731(2)	136	*x, -1+y, z*
C14	H14a	Cg(C8-C13)	0.99	2.94	3.754(2)	140	*1-x, 1-y, 1-z*
6							
O3	H3o	O1	0.84(4)	1.91(4)	2.646(4)	145(4)	*x, y, z*
C1	H1a	O3	0.98	2.60	3.403(5)	139	*x, 1½-y, ½+z*

File Name
Julio_rev.docx

Date
09.11.2017

Page
14 (15)

Conclusions

The novel electrolyses products, **5** and **6**, were generated by electro-reductive cleavage of **4**. These are diastereoisomeric, differing in the configurations at the methine-C6 and -C7 atoms, i.e. of opposite chirality in **5** and with the same chirality in **6**. This has a profound influence on the molecular conformation of the central, eight-membered, –C(H)–C(H)–C⬛C–(CH$_2$)$_2$–C⬛C, which approximates a boat in **5** and a chair in **6**. The generation of the eight-membered ring appended to a cyclopentenyl ring as found in **5** and **6** has no precedents in the crystallographic literature suggesting electrochemical-mediated synthesis offers opportunities in synthetic organic chemistry.

References

[1]   M. F. Nielsen, J. H. P. Utley, *"Reductive Coupling"* in *Organic Electrochemistry*. H. Lund, O. Hammerich (Eds), 4th Edition, Marcel Dekker, Chapter 21, pp. 795, **2001**.

[2]   I. Fussing, M. Gullu, O. Hammerich, A. Hussain, M. F. Nielsen, J. H. P. Utley, *J. Chem. Soc. Perkin Trans. 2* **1996**, p. 649.

[3]   I. Fussing, O. Hammerich, A. Hussain, M. F. Nielsen, J. H. P. Utley, *Acta Chem. Scand.* **1998**, *52*, 328.

[4]   S. U. Pedersen, T. Lund, K. Daasbjerg, M. Pop, I. Fussing, H. Lund, *Acta Chem. Scand.* **1998**, *52*, 657.

[5]   J. Andersson, L. Eberson, *J. Chem. Soc. Chem. Commun.* **1976**, p. 565.

[6]   J. Andersson, L. Eberson, C. Svenssson, *Acta Chem. Scand.* **1978**, *B32*, 234.

[7]   E. L. Eliel, D. E. Rivard, *J. Org. Chem.* **1952**, *17*, 1252.

[8]   J. Nosek, *Coll. Czech. Chem. Comm.* **1964**, *29*, 592.

[9]   K. Hannemanm, J. Wirz, A. Riesen, *Helv. Chim. Acta* **1988**, *71*, 1841.

[10]   E. D. Bergmann, Z. Pelchwicz, *J. Am. Chem. Soc.* **1953**, *75*, 4281.

[11]   L. F. Tietze, Th. Eicher, *Reactions and Syntheses in the Organic Chemistry Laboratory*. D. Ringe (translator), University Science Books p. 89, **1989**.

[12]   A. I. Vogel, *Textbook of Practical Organic Chemistry*. Longman. 5th edition, p. 1040, **1996**.

[13]   CrystalClear. User Manual. Rigaku/MSC Inc., Rigaku Corporation, The Woodlands, TX, **2005**.

[14]   T. Higashi, ABSCOR. Rigaku Corporation, Tokyo, Japan, **1995**.

[15]   G. M. Sheldrick, *Acta Crystallogr. A* **2008**, *64*, 112.

[16]   G. M. Sheldrick, *Acta Crystallogr. C* **2015**, *71*, 3.

[17]   L. J. Farrugia, *J. Appl. Crystallogr.* **2012**, *45*, 849.

[18]   A. L. Spek, *J. Appl. Crystallogr.* **2003**, *36*, 7.

[19]   K. Brandenburg, DIAMOND. Crystal Impact GbR, Bonn, Germany, **2006**.

[20]   J. Gans, D. Shalloway, *J. Molec. Graphics Model.* **2001**, *19*, 557.

[21]   J. P. Petrovich, J. D. Anderson, M. M. Baizer, *J. Org. Chem.* **1966**, *31*, 3897.

[22]   R. M. Scrowston, D. C. Shaw, *J. Chem Soc. Perkin Trans 1* **1976**, *7*, 749.

[23]   S. K. Wolff, D. J. Grimwood, J. J. McKinnon, M. J. Turner, D. Jayatilaka, M. A. Spackman, University of Western Australia, **2012**.

[24]   C. R. Groom, I. J. Bruno, M. P. Lightfoot, S. C. Ward, *Acta Crystallogr. B* **2016**, *72*, 171.

[25]   J. Wang, M. Wang, J. Xiang, H. Xi, A. Wu, *Tetrahedron*, **2015**, *71*, 7687.

[26]   M. Nishio, *Phys. Chem. Chem. Phys*. 2011, *13*, 13873-13900.